Lumped Interconnect Models Via Gaussian Quadrature

Keith Nabors, Tze-Ting Fang, Hung-Wen Chang and Kenneth S. Kundert
Cadence Design Systems, San Jose, California
Jacob K. White
Massachusetts Institute of Technology, Cambridge, Massachusetts

Abstract

This paper presents a new Gaussian quadrature method for interconnect modeling which applies to one-dimensional distributions of circuit element values, the line structures often used to model interconnect wires. The method takes a line circuit, which may be an arbitrary combination of lumped and distributed elements, and produces a small lumped model whose transfer and input characteristics approximately match those of the original circuit. The same algorithm may be used to generate lumped models for distributed elements, or to reduce long chains of lumped elements. The method also applies to one-dimensional distributions of coupling circuit elements, and, in general, to any one-dimensional distribution of circuit element quantities. Several examples demonstrate that the quadrature-based method is capable of automatically generating compact RC, LC and RLC line models with arbitrary accuracy.

1 Introduction

The need for accurate yet efficient interconnect models for timing and other performance verification has motivated many modeling techniques. Perhaps the most fruitful approach taken is matching time moments of the interconnect's output waveforms, a technique pioneered for circuit analysis by Elmore [5] and later generalized in different ways [10, 15, 17, 14]. Several specializations of the general moment matching techniques provide efficient methods for analyzing RC trees, transmission lines and related special cases [16, 20, 23, 3], while the newer Krylov methods offer more robust general algorithms for moment matching [6, 21, 13, 2]. Apart from moment matching, analytical methods may be applied in certain special cases [19].

This paper presents a new method for interconnect modeling which applies only to one-dimensional distributions of circuit element values, the structures often used to model interconnect wires. The method takes a line circuit, which may be an arbitrary combination of lumped and distributed elements, and produces a small lumped line circuit whose transfer and input characteristics approximately match those of the original circuit. The same algorithm may be used to generate lumped models for distributed elements, or to reduce long chains of lumped elements. The method also applies to one-dimensional distributions of coupling capacitances and inductances.

The new method works by preserving the way the elements are arranged along the original line in the small lumped model. By matching the moments of the original circuit-element distribution to the moments of the lumped model, the algorithm indirectly preserves the response of the line. The moments that are matched explicitly by the algorithm are the moments of the circuit-element distribution, or taper, of the line, not the time moments of any response. Intuitively such an approach works because any voltage or current along the line sees a similar distribution of circuit elements in either the original line, or the small lumped model. The matching of the taper's moments can be done efficiently using Gaussian quadrature, which also guarantees positive elements in the final model. Thus the resulting wire models are always stable, regardless of how they are interconnected.

The new method differs from other lumped-circuit approximation techniques which are typically based on preserving the time response or moments of time responses [24, 8, 1, 12], or use uniform lumps, or other techniques [9]. One of the more interesting properties of the new method is its ability to simultaneously match both transfer and input characteristics in an easily used circuit model. This allows it to be useful even for relatively low-loss lines. Also, the method generates the identical line model for a long line when applied directly to the long line, or when first applied to sections of the line, and then to the series composition of the resulting section models. This composition property ensures that the model accuracy is not compromised when the method is used to reduce different pieces of extracted layout as they are generated, and then applied again to the composition of the models, as is often convenient in practice.

Section 2 uses the transmission line equations to show how preserving a line's taper preserves its electrical behavior, motivating the development of the Gaussian-quadrature procedure of Section 3 for preserving the taper in the model by matching element-distribution moments. Section 3.1 develops the algorithm for the special case of RC lines, but the results apply directly to any line made up of two kinds of elements. Section 3.2 shows how matching element-distribution moments leads to time-moment matching for RC lines, and Section 3.3 discusses the composition property. The results in Section 4 are aimed at comparing the new method to uniform lumping for RC, LC and RLC lines.

2 Transmission Line Equations

A simple transformation of the RLCG transmission line equations shows why matching a line's distributed-element taper preserves the line's time response. The Laplace transforms of the voltage, $V(s,z)$, and current, $I(s,z)$, for complex frequency s and transmission line position z are related by the set of ordinary differential equations (see, for example, [11])

$$\frac{d}{dz}V(s,z) = -[r(z)+sl(z)]I(s,z);$$

DAC 97, Anaheim, California
©1997 ACM 0-89791-920-3/97/06..$3.50

$$\frac{d}{dz}I(s,z) = -[g(z)+sc(z)]V(s,z), \quad (1)$$

where $r(z)$, $l(z)$, $g(z)$ and $c(z)$ are the per-unit-length series resistance, series inductance, shunt conductance and shunt capacitance, respectively, at z. The accumulated resistance along the line at z may be written

$$R(z) = \int_0^z r(y)dy, \quad (2)$$

assuming that $z = 0$ at one end of the line. In the case where $r(z)$ is non-zero, the accumulated capacitance along the line may be written as a function of R since $R(z)$'s monotonicity implies the existence of the inverse function $z(R)$. In particular, it is possible to define $C(\cdot)$ as

$$C(R) = \int_0^{z(R)} c(y)dy. \quad (3)$$

Similarly,

$$L(R) = \int_0^{z(R)} l(y)dy; \; G(R) = \int_0^{z(R)} g(y)dy.$$

Using these new definitions and the Chain Rule allows (1) to be rewritten as

$$\begin{aligned} \frac{dV}{dR} &= -\left[1+s\frac{dL}{dR}\right]I; \\ \frac{dI}{dR} &= -\left[\frac{dG}{dR}+s\frac{dC}{dR}\right]V. \end{aligned} \quad (4)$$

These equations indicate that lines with identical $dL(R)/dR$, $dC(R)/dR$ and $dG(R)/dR$ values lead to identical solutions if R is used as the spatial variable. The solutions as functions of distance along the line, $V(s,z)$ and $I(s,z)$, are not necessarily the same. However, the solutions must match at the terminals since changing variables between R and z leaves the endpoint values untouched.

The important special case of RC lines is treated by setting $L = G = 0$ in (4), indicating that RC lines with identical $dC(R)/dR$ values are electrically equivalent [18]. LC lines are governed by equations of the same form as the RC case, with L playing the role of R. In general there are several ways of eliminating the spatial variable z, but all lead to the conclusion that preserving the taper of the line preserves terminal behavior. These arguments generalize to coupled lines by replacing the distributed element functions $r(z)$, $c(z)$, $l(z)$ and $g(z)$ with matrices, and the current I and voltage V with vectors.

3 Matching Two-Element Lines

Equation (4) suggests that the line-circuit reduction problem may be solved by finding simpler element distribution functions that approximate the original line's element distribution functions. This section develops a Gaussian-quadrature procedure for generating lumped-model approximations for lines with two kinds of circuit elements by matching moments of the element distribution functions. Although the algorithm presentation uses RC lines as a concrete example, Section 4 demonstrates that the Gaussian-quadrature method applies directly to other two-element lines (for example LC lines), and may be used repeatedly to generate models for lines made with more than two elements types (for example RLC lines).

3.1 RC Line Matching

As a concrete example, consider the approximation of an RC line's capacitance taper, $c(R) = dC(R)/dR$, with R_t equal to the total resistance of the line. The RC line may be lumped or distributed, or an arbitrary combination of both. Since the cumulative capacitance distribution function, $C(R)$, is always monotonic increasing, finding an approximate taper, $\hat{c}(R)$, that preserves the first few moments of $c(R)$,

$$\int_0^{R_t} \hat{c}(R)R^k dR = \int_0^{R_t} c(R)R^k dR, \; k = 0, 1\ldots, 2m-1, \quad (5)$$

for some chosen m, is a viable approach. Forcing $\hat{c}(R)$ to correspond to a lumped circuit makes it impulsive,

$$\hat{c}(R) = \sum_i \hat{c}_i \delta(R - \hat{R}_i), \quad (6)$$

where $\hat{c}_i$ is the value of the i-th lumped capacitor, positioned $\hat{R}_i$ away from the reference end of the line. Substituting (6) into (5) gives

$$\int_0^{R_t} c(R)R^k dR = \sum_i \hat{c}_i \hat{R}_i^k, \; k = 0, \ldots, 2m-1. \quad (7)$$

Algorithm 1 (Quadrature for $\int_a^b \omega(x)f(x)dx$)

Find Orthogonal Polynomials (Gram-Schmidt)
Comment: $(f,g) \equiv \int_a^b \omega(x)f(x)g(x)dx$.
Initialize $p_0(x) = 1$, $p_{-1}(x) = 0$, $\gamma_1^2 = 0$.
for $(i = 1$ to $i = m)$ {
  Set $\delta_{i+1} = (xp_i, p_i)/(p_i, p_i)$.
  If $i > 0$, **set** $\gamma_{i+1}^2 = (p_i, p_i)/(p_{i-1}, p_{i-1})$.
  Set $p_{i+1}(x) = (x - \delta_{i+1})p_i(x) - \gamma_{i+1}^2 p_{i-1}(x)$.
}

Find Weights and Abscissas
Calculate the eigenvalues, λ_i, $i = 1, \ldots, m$, of the tridiagonal matrix,

$$J = \begin{bmatrix} \delta_1 & \gamma_2 & & \\ \gamma_2 & \ddots & \ddots & \\ & \ddots & \ddots & \gamma_m \\ & & \gamma_m & \delta_m \end{bmatrix}.$$

Set $\hat{x}_i = \lambda_i$, $i = 1, \ldots, m$.
Calculate the eigenvectors of J, y_i, $i = 1, \ldots, m$.
Normalize y_i, $i = 1, \ldots, m$, so $y_i^T y_i = (p_0, p_0)$.
Set $w_i = (y_i[1])^2$, first entry squared, $i = 1, \ldots, m$.

Return x_i and w_i, $i = 1, \ldots, m$.

In this special case, the moment-matching condition is efficiently satisfied by approximating the $c(R)$ integral using Gaussian quadrature (see, for example, [22]). Gaussian quadrature provides a procedure for approximating integrals by weighted sums,

$$\int_a^b \omega(x)f(x)dx \approx \sum_i w_i f(x_i) = \int_a^b \sum_i w_i \delta(x - x_i)f(x)dx. \quad (8)$$

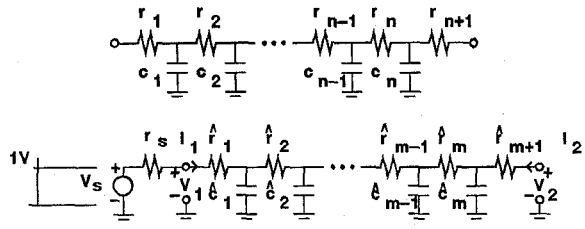

Figure 1: The form of the original (top) and approximate (bottom) RC line when applying Algorithm 2.

The approximation is exact when $f(x)$ has the form x^k, $k = 0, 1, \ldots, 2m-1$ [22]. Thus (7) may be enforced by applying the Gaussian quadrature rule (8) with $\omega(x) \to c(R)$, $a \to 0$, and $b \to R_t$. The weight, w_i, is interpreted as the i-th lumped capacitor value, $\hat{c}_i$, and the corresponding abscissa, x_i, is the i-th lumped capacitor's resistive position on the line, $\hat{R}_i$.

Algorithm 2 (RC Reduction by quadrature)

Set m to desired number of reduced-line capacitors. If the original line is an n capacitor lumped line, choose $m \leq n$.
Calculate the Gaussian quadrature approximation, $\int_0^{R_t} c(R)f(R)dR \approx \int_0^{R_t} \sum_{i=1}^{m} \hat{c}_i \delta(R - \hat{R}_i) f(R)dR$, using Algorithm 1.
Identify $\hat{c}_i$ as the i-th capacitor with position $\hat{R}_i$ on the reduced line.

Algorithm 1 calculates the approximation (8) by Gaussian quadrature. Algorithm 2 applies Algorithm 1 to calculate a reduced lumped RC line model of the form (6) for an original RC line with taper $c(R)$. Under certain regularity conditions on $c(R)$, Algorithm 1 as applied in Algorithm 2 always produces positive $\hat{c}_i$ values [22]. The orthogonalization properties of Gaussian quadrature further guarantee that when the original line in Algorithm 2 is lumped and $m = n$, the reduced line is identical to the original line.

Assuming reuse of inner products, the cost of the Gram-Schmidt part of Algorithm 1 applied to an n capacitor RC line to calculate an m capacitor reduced RC line requires approximately $2n$ flops for each δ calculation and $2n$ more flops for each pass through the Gram-Schmidt loop for a total of $4mn$ flops. Since J in Algorithm 2 is symmetric, tridiagonal, the weight and abscissa calculation requires about $24m^2$ flops by the symmetric QR algorithm [4], so the complete Algorithm 1 calculation requires roughly $4mn + 24m^2$ flops. In practice, $n > m$ by a large enough margin so the complete calculation is $O(mn)$.

3.2 Connections to Time Moments

For the reduction illustrated in Figure 1, the first three moments matched by Algorithm 2 are

$$q_0 = \sum_{i=1}^{n} c_i;\ q_1 = \sum_{i=1}^{n} R_i c_i;\ q_2 = \sum_{i=1}^{n} R_i^2 c_i.$$

Here $R_i = \sum_{j=1}^{i} r_j$ is the cumulative resistance up to node i starting at the left port in Figure 1, following the notation of Algorithm 2. The source resistance, r_s, is taken as zero throughout this section for simplicity. These first few taper moments have physical meaning: q_0 is the total capacitance, while q_1 and q_2 are proportional to the total charge and total energy stored in the steady state when the circuit is presented with the boundary conditions of a step response admittance test. The first moments of the voltage response for the original RC line are [10, 24]

$$m_{1V}^1 = \sum_{i=1}^{n} R_i c_i = q_1;\ m_{1V}^2 = \sum_{i=1}^{n} (R_t - R_i)c_i = R_t q_0 + q_1,$$

while the first moments of the input current response with the output shorted are

$$m_{1I}^1 = q_2/R_t^2;\ m_{1I}^2 = q_0 - 2q_1/R_t + q_2/R_t^2.$$

Here the superscript indicates the driven port number, as in Figure 1, and the subscript indicates the moment order and type. Since Algorithm 2 preserves q_0, q_1 and R_t, it also preserves these moments, and the corresponding zeroth-order moments.

3.3 Composition Property

In many interconnect analysis strategies, reduced line pieces are combined to form longer lines, trees or meshes depending on the overall topology, and the composed circuits may be large enough to require additional reduction. The obvious difficulty with such a nested reduction strategy is that reduction errors are likely to accumulate.

In the special case of connecting line pieces reduced using Algorithm 2 in series to form a longer line, and then reducing the composed line again by Algorithm 2, the resulting line is identical to the one produced by reducing the longer line directly. This implies that there is no accuracy penalty for using this method successively in on-the-fly reduction. The result can be thought of as a generalization of the first-moment preserving approach in [24].

Theorem 1 *Consider two RC lines, characterized by $c^A(R)$ and $c^B(R)$ on the intervals $[0, R_t^A]$ and $[0, R_t^B]$ respectively. If $\hat{c}_A(R)$ and $\hat{c}_B(R)$ are m^{th}-order lines produced by Algorithm 2, then the m^{th}-order reduction of the composition of $c^A(R)$ and $c^B(R)$ produced by Algorithm 2 can be precisely computed by applying Algorithm 2 to the composition of $\hat{c}_A(R)$ and $\hat{c}_B(R)$* ∎.

The proof of Theorem 1 is omitted for brevity.

4 Results

Algorithm 2 applies directly to RC line circuits, and may be used to generate approximate LC line models with inductance replacing resistance. Lines with more than two element types require repeated application of Algorithm 2 to the different element distributions. RLC lines, for example, may be approximated by first using Algorithm 2 to obtain lumped models for $l(R)$ and $c(R)$ separately, and then merging the two on a single set of resistors.

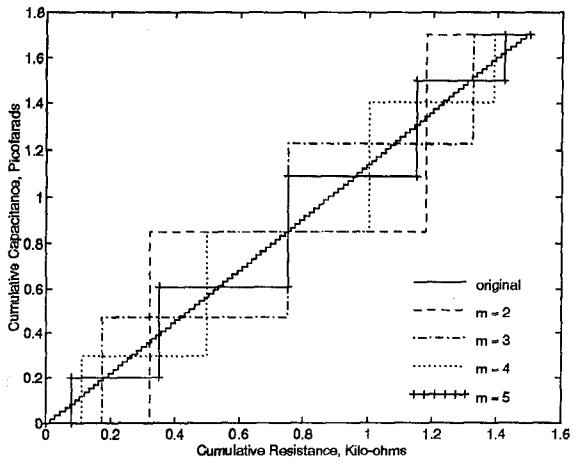

Figure 2: The original and approximate tapers generated by Algorithm 2 for the uniform lumped RC test line.

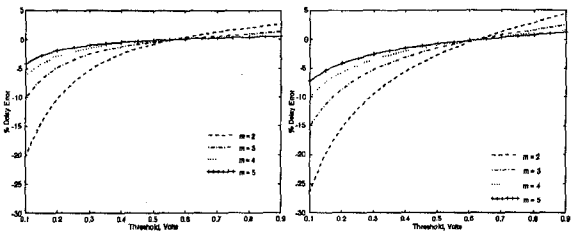

Figure 3: The percentage delay error for the approximate lines of Figure 2 (left) and for uniform-lump approximations with the same number of capacitors, m (right).

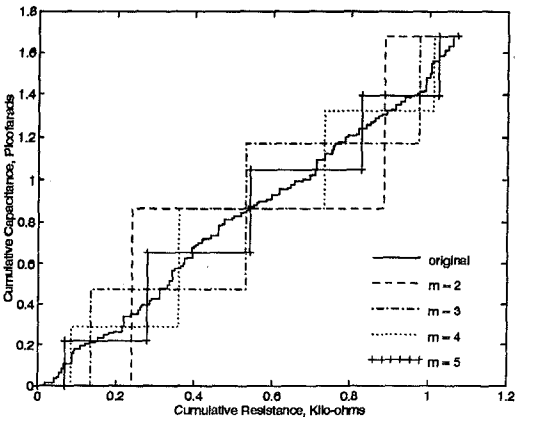

Figure 5: The original and approximate tapers for the random lumped RC test line.

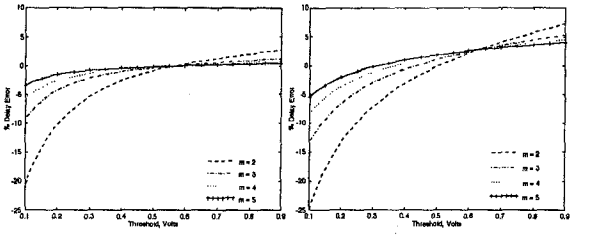

Figure 6: The percentage delay error for the approximate lines of Figure 5 (left) and for uniform-lump approximations with the same number of capacitors, m (right).

4.1 RC Lines

Figure 2 illustrates the $C(R)$ function for the original uniform lumped line of the form pictured in Figure 1, together with the approximate tapers produced using Algorithm 2 for various numbers of capacitors, m. The original line has $r_i = 1500/101\Omega$, $c_i = 1700/100\text{fF}$ and $n = 100$.

Applying a unit voltage step to both the original and approximate lines as illustrated in Figure 1, with $r_s = 150\Omega$, produces output voltage delay and input source current differences pictured in Figures 3 and 4 respectively. For a given number of capacitors, the superiority of Algorithm 2 over uniform lumped models is evident.

Figure 5 illustrates the taper of a second RC line example with random resistances uniformly distributed between 1.48514Ω and 2.22772Ω, and random capacitances uniformly distributed between 1.7fF and 25.5fF arranged in the topology of Figure 1 with $n = 100$. Also ten randomly chosen resistors are set to 5Ω in an attempt to model vias, and ten randomly chosen capacitors are set to 50fF to represent load capacitances. Applying Algorithm 2 to the random line gives the element tapers in Figure 5. The uniform lumped lines used for comparison have element values calculated from $R_t = 1070.87\Omega$ and $C_t = 1.68132\text{pF}$.

Applying a unit voltage step to both the original and approximate lines as illustrated in Figure 1, with $r_s = 150\Omega$, produces output voltage delay and input source current differences pictured in Figures 6 and 7 respectively. Algorithm 2 retains its superior delay and input impedance properties for the more realistic random line test case.

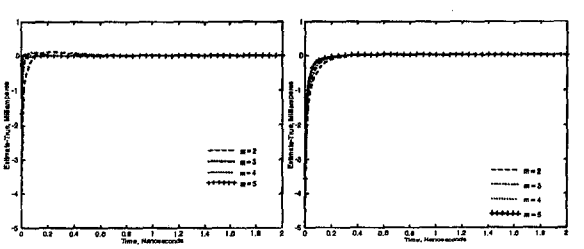

Figure 4: The voltage source current error for the approximate lines of Figure 2 (left) and for uniform-lump approximations with the same number of capacitors, m (right).

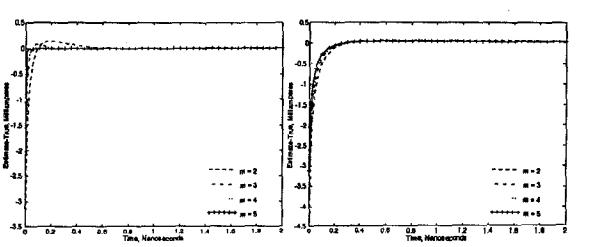

Figure 7: The voltage source current error for the approximate lines of Figure 5 (left) and for uniform-lump approximations with the same number of capacitors, m (right).

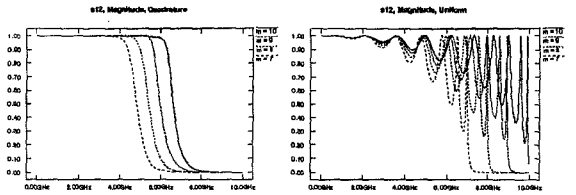

Figure 8: The magnitude of the transmission scattering parameter, s12, for the example LC line approximated by Gaussian quadrature (right) and uniform lumping (left).

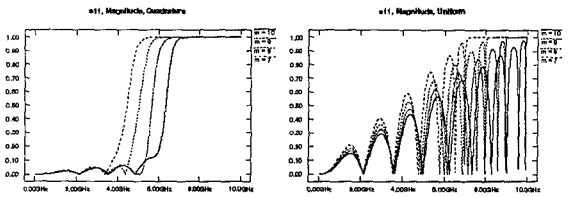

Figure 9: The magnitude of the reflections scattering parameter, s11, for the example LC line approximated by Gaussian quadrature (right) and uniform lumping (left).

4.2 LC Lines

Algorithm 2 applies directly to lumped LC line reduction if the resistances are replaced with inductances. Then $c(L)$ replaces $c(R)$, and $c(L)$ need not be lumped as implied in the statement of Algorithm 2. In particular, an ideal delay line with total inductance L_t and total capacitance C_t may be approximated by setting $c(L) = C_t/L_t$ and applying Gaussian quadrature as in Algorithm 2. The resulting lumped elements are scaled versions of the tapers in Figure 2, the only difference being due to the lumped nature of the original line taper in Figure 2.

Figures 8 and 9 illustrate the magnitudes of the scattering parameters for such an approximation of a uniform, distributed, 50mm, 300ps delay, LC line with $z_0 = 50\Omega$, $C_t = 6.67$pF and $L_t = 16.67$nH. Driving either end of the line through a 50Ω termination, and shorting the other end with a 50Ω resistor gives the illustrated scattering parameters. The original line's characteristics of s11 = 0, s12 = 1 and linear phase are not plotted in the figures.

In general the Gaussian quadrature approximation trades off usable bandwidth for diminished reflections. This is evident, for example, when comparing the lumped and quadrature approximations in Figure 8. The frequency where the uniform lumped model becomes an open circuit for $m = 10$ is around 10GHz, while for the quadrature model it is only 7GHz. On the other hand, the lumped model s12 indicates significant attenuation around 3GHz, while the quadrature model remains useful to 6GHz. Thus the quadrature model may be used when the driving signals have most of their energy below a certain frequency, and this frequency is higher than for the uniform model with the same number of lumps. The plots also show that the quadrature models eventually end up having significant ripples before the band edge as m is increased. The ripples are not eliminated, but rather postponed. Phase plots are not included due to space restrictions, but the phase characteristics exhibit the same bandwidth trade-off as the magnitudes.

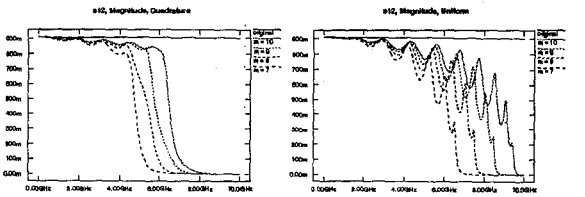

Figure 10: The magnitude of the transmission scattering parameter, s12, for the example RLC line approximated by Gaussian quadrature (right) and uniform lumping (left).

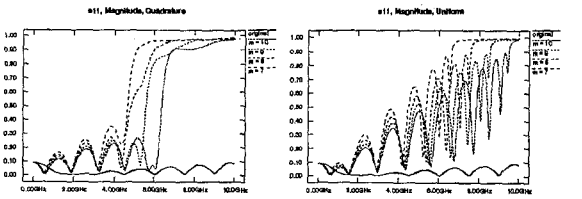

Figure 11: The magnitude of the reflections scattering parameter, s11, for the example RLC line approximated by Gaussian quadrature (right) and uniform lumping (left).

4.3 RLC Lines

Applying Algorithm 2 first with $c(R)$, and then replacing $c(R)$ by $l(R)$ and using Algorithm 2 again, gives a capacitance and inductance taper on a common resistive spine. Merging the two so that the inductors and capacitors see the same resistances as they would separately gives an method for approximating RLC lines.

Figures 10 and 11 give the scattering parameter data for models of a uniform RLC line identical to the LC line of the previous section, but with a uniform distributed resistance of $R_t = 10\Omega$, instead of zero. The same trade off between bandwidth and fidelity is evident in this low-loss example, and the match to the original data is poorer. The original line data in these plots was calculated from a uniform one-hundred-lump approximation.

5 Conclusions and Future Work

The recasting of the line-matching problem into one of matching element-distribution function moments sheds a different light on earlier work motivated by matching time moments. For the RC line case Algorithm 2 is most similar to the many methods for preserving Elmore delay during circuit-to-circuit reduction described in [24] and its references. Applying those methods to RC lines typically preserves total resistance and capacitance together with Elmore delay, which amounts to preserving the first few spatial moments of the RC line taper. More recent work in this area also preserves moments computed at infinite frequency [1, 7]. For an RC line the grounded capacitors become shorts in the infinite frequency limit, so this kind of technique preserves the resistances near the terminals, as does Algorithm 2. The older techniques have the advantage of applying to more general RC circuits than Algorithm 2, but Algorithm 2 has unique convergence and composability properties.

Despite previous methods' applicability to more general RC circuits than just RC lines, their ties to time moments make it difficult to find generalizations to circuits with other kinds of circuit elements. In contrast, Algorithm 2 applies

directly to LC and RLC circuits since it matches element distribution functions, not time waveforms. By repeated application of Algorithm 2 to the individual element distribution functions of a line relative to a chosen index distribution, it is possible to construct lumped models for any lumped or distributed line circuit constructed with any kind of element type. The element types need not be just inductance, capacitance and resistance, but could be ideal delays, skin-effect elements, or any other type of element.

More work is needed to determine if models constructed this way are useful. The results of this paper, for example, indicate that the method works better for RC and LC lines than for low-loss RLC lines. At this writing it is not clear why the no-loss LC models perform better than the RLC models, given the good performance of the maximum-loss RC models. It is also not clear how well coupled models generated by applying Algorithm 2 to coupling distributions would perform.

The authors would like to acknowledge helpful conversations with Ricardo Telichevesky, Xiaojun Zhu and Steve McCormick.

REFERENCES

[1] Carsten Borchers, Burkhard Ludwig, and Erich Barke. Reduction parasitärer RC-netzwerke in höchstintegrierten schaltungen. In *6th E.I.S. Workshop*, 1993.

[2] J. Eric Bracken. Algorithms for passive modeling of linear interconnect networks. To apper in IEEE Transactions on Circuits and Systems.

[3] J. Eric Bracken, Vivek Raghavan, and Ronald A. Roher. Interconnect simulation with asymptotic waveform evaluation (AWE). *IEEE Transactions on Circuits and Systems—I: Fundamental Theory and Applications*, 39(11):869–878, November 1992.

[4] Germund Dahlquist and Åke Björck. *Numerical Methods*. Prentice-Hall, Englewood Cliffs, 1974.

[5] W. C. Elmore. The transient response of damped linear networks with particular regard to wideband amplifiers. *Journal of Applied Physics*, 19:55–63, January 1948.

[6] Peter Feldmann and Roland W. Freund. Efficient linear circuit analysis by padé approximation via the lanczos process. *IEEE Transactions on Computer-Aided Design of Integrated Circuits and Systems*, 14(5):639–649, May 1995.

[7] Martin Frerichs, July 1996. Personal communication.

[8] Nanda Gopal, Dean P. Neikirk, and Lawrence T. Pillage. Evaluating RC-interconnect using moment-matching approximations. In *IEEE/ACM International Conference on Computer Aided Design Digest of Technical Papers*, pages 74–77, 1991.

[9] Rohini Gupta, Seok-Yoon Kim, and Lawrence T. Pileggi. Domain characterization of transmission line models and analyses. *IEEE Transactions on Computer-Aided Design of Integrated Circuits and Systems*, 15(2):184–193, February 1996.

[10] Mark A. Horowitz. *Timing Models for MOS Circuits*. PhD thesis, Stanford Univeristy, January 1984.

[11] William H. Hyat, Jr. *Engineering Electromagnetics*. McGraw-Hill, New York, third edition, 1974.

[12] Andrew B. Kahng and Sudhakar Muddu. Efficient analyses and models of VLSI and MCM interconnects. Submitted to IEEE Transactions on VLSI Systems.

[13] Kevin J. Kerns, Ivan L. Wemple, and Andrew T. Yang. Stable and efficient reduction of substrate model networks using congruence transforms. In *IEEE/ACM International Conference on Computer Aided Design Digest of Technical Papers*, pages 207–214, 1995.

[14] Haifang Liao and Wayne Wei Ming Dai. Capturing time-of-Flight delay for transient analysis based on scattering parameter macromodel. In *IEEE/ACM International Conference on Computer Aided Design Digest of Technical Papers*, pages 412–417, 1994.

[15] Steven Paul McCormick. *Modeling and Simulation of VLSI Interconnections with Moments*. PhD thesis, Massachusetts Institute of Technology, June 1989.

[16] Peter R. O'Brien and Thomas L. Savarino. Efficient on-chip delay estimation for leaky models of multiple-source nets. In *Proc. IEEE Custom Integrated Circuits Conference*, pages 9.6.1–9.6.4, 1990.

[17] Lawrence T. Pillage and Ronald A. Roher. Asymptotic waveform evaluation for timing analysis. *IEEE Transactions on Computer-Aided Design of Integrated Circuits and Systems*, 9(4):352–366, April 1990.

[18] E. N. Protonotarios and O. Wing. Theory of nonuniform RC lines, Part I: Analytic properties and realizability conditions in the frequency domain. *IEEE Transactions on Circuit Theory*, 14(1):2–12, March 1967.

[19] Vasant B. Rao. Delay analysis of the distributed rc line. In *Proc. of the 32nd Design Automation Conference*, pages 370–375, 1995.

[20] Curtis L. Ratzlaff, Nanda Gopal, and Lawrence T. Pillage. RICE: Rapid interconnect circuit evaluator. In *Proc. of the 28th Design Automation Conference*, pages 555–566, 1991.

[21] L. M Silveira, M. Kamon, and J. K. White. Direct computation of reduced-order models for circuit simulation of 3-d interconnect structures. In *Proceedings of the 3nd Topical Meeting on Electrical Performance of Electronic Packaging*, pages 254–248, Monterey, California, November 1994.

[22] J. Stoer and R. Bulirsch. *Introduction to Numerical Analysis*. Springer-Verlag, New York, 1980.

[23] Tak K. Tang and Michel S. Nakhla. Analysis of high-Speed VLSI interconnects using the asymptotic waveform evaluation technique. *IEEE Transactions on Computer-Aided Design of Integrated Circuits and Systems*, 11(3):341–352, March 1992.

[24] Paul Vanoostende, Paul Six, and Hugo J. De Man. DARSI: RC data reduction. *IEEE Transactions on Computer-Aided Design of Integrated Circuits and Systems*, 10(4):493–500, April 1991.